



NO₂ seasonal evolution in the North Subtropical free troposphere

M. Gil-Ojeda et al.

This discussion paper is/has been under review for the journal Atmospheric Chemistry and Physics (ACP). Please refer to the corresponding final paper in ACP if available.

NO₂ seasonal evolution in the North Subtropical free troposphere

M. Gil-Ojeda¹, M. Navarro-Comas¹, L. Gómez-Martín¹, J. A. Adame¹,
A. Saiz-Lopez², C. A. Cuevas², Y. González³, O. Puentedura¹, E. Cuevas³,
J.-F. Lamarque⁴, D. Kinninson⁴, and S. Tilmes⁴

¹Instituto Nacional de Técnica Aeroespacial, Torrejón de Ardoz, Spain

²Atmospheric Chemistry and Climate Group, Institute of Physical Chemistry Rocasolano, CSIC, Madrid, Spain

³Izaña Atmospheric Research Center, AEMET, Tenerife, Spain

⁴Atmospheric Chemistry Division, NCAR, Boulder, CO, USA

Received: 20 February 2015 – Accepted: 4 May 2015 – Published: 22 May 2015

Correspondence to: M. Gil-Ojeda (gilm@inta.es)

Published by Copernicus Publications on behalf of the European Geosciences Union.

Title Page

Abstract

Introduction

Conclusions

References

Tables

Figures



Back

Close

Full Screen / Esc

Printer-friendly Version

Interactive Discussion



Abstract

Three years of Multi-Axis Differential Optical Absorption Spectroscopy (MAXDOAS) measurements (2011–2013) have been used for estimating the NO_2 mixing ratio along a horizontal line of sight from the high mountain Subtropical observatory of Izaña, at 2370 m.a.s.l. (NDACC station, 28.3°N , 16.5°W). The method is based on horizontal path calculation from the $\text{O}_2\text{--O}_2$ collisional complex at the 477 nm absorption band which is measured simultaneously to the NO_2 , and is applicable under low aerosols loading conditions.

The MAXDOAS technique, applied in horizontal mode in the free troposphere, minimizes the impact of the NO_2 contamination resulting from the arrival of MBL air masses from thermally forced upwelling breeze during central hours of the day. Comparisons with in-situ observations show that during most of measuring period the MAXDOAS is insensitive or very little sensitive to the upwelling breeze. Exceptions are found during pollution events under southern wind conditions. On these occasions, evidence of fast efficient and irreversible transport from the surface to the free troposphere is found.

Background NO_2 vmr, representative of the remote free troposphere, are in the range of 20–45 pptv. The observed seasonal evolution shows an annual wave where the peak is in phase with the solar radiation. Model simulations with the chemistry-climate CAM-Chem model are in good agreement with the NO_2 measurements, and are used to further investigate the possible drivers of the NO_2 seasonality observed at Izaña.

1 Introduction

Nitrogen oxides play an important role in tropospheric chemistry as they control the O_3 photochemical catalytic production (Crutzen, 1979), the abundance of hydroxyl radicals, and contribute to the nitrate aerosols formation. In a background unpolluted atmosphere where NO_x concentrations are low, net ozone loss occurs during photochemically active periods (Liu et al., 1983; Isaksen et al., 2005). NO_x abundance is

ACPD

15, 14473–14504, 2015

NO_2 seasonal evolution in the North Subtropical free troposphere

M. Gil-Ojeda et al.

Title Page

Abstract

Introduction

Conclusions

References

Tables

Figures

◀

▶

◀

▶

Back

Close

Full Screen / Esc

Printer-friendly Version

Interactive Discussion



NO₂ seasonal evolution in the North Subtropical free troposphere

M. Gil-Ojeda et al.

Title Page

Abstract

Introduction

Conclusions

References

Tables

Figures

◀

▶

◀

▶

Back

Close

Full Screen / Esc

Printer-friendly Version

Interactive Discussion



highly variable since it is influenced by non-steady natural and anthropogenic emissions and its global distribution is still uncertain. Free Troposphere (FT) source inventories indicate that major production comes from lighting ($2\text{--}16\text{ Tg N yr}^{-1}$), followed by NH_3 oxidation ($0.3\text{--}3\text{ Tg N yr}^{-1}$), stratospheric intrusion ($0.08\text{--}1\text{ Tg N yr}^{-1}$) and aircraft ($0.6\text{--}0.7\text{ Tg N yr}^{-1}$). Contribution from the boundary layer in remote regions is rare (Bradshaw et al., 2000).

Information of surface NO_x on polluted areas is available due to extended governmental air quality networks. During the last decade, satellite instruments have demonstrated capabilities for successful retrieval of tropospheric NO_2 identifying enhanced concentrations over urban and industrial areas in the boundary layer (Richter et al., 2005; Irie et al., 2005) and tracking the temporal trends (Hilboll et al., 2013; Cuevas et al., 2014). However, direct NO_2 measurements in the background FT are scarce due to the requirement of observational platforms above, typically 2000 m.a.s.l., but also due to the low concentrations present at those levels.

Airborne NO_2 measurements have been performed for decades (Ridley et al., 1988; Carroll et al., 1990), however the need for very short response times at concentrations close to the instrumental detection limit, make the FT observations a challenging task. Even though well characterized aircraft instruments reach detection limits as low as 10 pptv (Heland et al., 2002), few studies are reported in the literature. Measurements are generally collected during individual field campaigns associated to specific targets such as chemistry missions or satellite validations (Jacob et al., 2003; Bucsela et al., 2008; Boersma et al., 2008; Baidar et al., 2013; Flynn et al., 2014). These time and space sparse data limit the study of seasonalities or trends in the FT. Only recently, attempts to obtain global FT NO_2 abundances from satellite OMI instrument has been performed for the first time (Choi et al., 2014) by using the cloud slicing technique (Ziemke, 2001). The method is based on the comparison of cloud and cloudless scenes to derive the FT mean concentrations. Results show that valuable information on NO_2 large scale phenomena can be derived on areas where clouds presence is frequent

but does not provide results in places such as East Atlantic subtropical latitudes where high pressures are dominant features.

Instruments operating in the few high mountain stations existent around the world are the only alternative to monitor NO_2 in the background FT. However, the in-situ measurements are often affected by the “upslope breeze effect” (Val Martin et al., 2008; Rodriguez et al., 2009; Reidmiller et al., 2010; Cuevas et al., 2013). Radiative heating in the mountain slopes result in air upwelling from the boundary layer contaminating the daytime measurements by generally larger values over the polluted lower layers.

Recently, Gomez et al. (2014) have presented a simple method based on a Modified Geometrical Approximation (MGA) to estimate trace gases concentrations at the level of the Izaña Observatory from MAXDOAS measurements. The horizontal path length is obtained from the oxygen collisional complex (O_4 , hereafter) simultaneously measured with the tracer under consideration (NO_2 and O_3). Gomez et al. examined a short summer period to demonstrate the validity of the method. Here we apply the same technique to data covering 3 full years (2011–2013) to analyze the seasonal evolution of the NO_2 concentrations in volume mixing ratio (vmr). MAXDOAS present two main advantages with respect to the in-situ instrument at this location, both related to the very long optical path of the measurements of over 60 km. Firstly, it minimizes the potential contribution of NO_2 that may be upwelled from the marine boundary layer (MBL). The breeze layer has a limited vertical extension and its relative contribution to the MAXDOAS long path is small. On the contrary, Izaña in-situ data around noon are strongly influenced by the underlying polluted MBL (Puentedura et al., 2012; Gomez et al., 2014). Secondly, due to the long light paths achieved by MAXDOAS in the FT, very low concentrations, of few ppt, can be measured.

Section 2 presents the method, limits and associated errors. In Sect. 3 the station and data sets are depicted. Section 4 describes the method used for profiles retrieval. The description of the chemical and back trajectories models is done in Sect. 5. Finally, Sects. 6 and 7 present the results and discussion, and summary, respectively.

NO_2 seasonal evolution in the North Subtropical free troposphere

M. Gil-Ojeda et al.

Title Page	
Abstract	Introduction
Conclusions	References
Tables	Figures
◀	▶
◀	▶
Back	Close
Full Screen / Esc	
Printer-friendly Version	
Interactive Discussion	



given by:

$$X_{\text{vmr}} = \frac{X_{\text{DSCD}}}{\frac{O_{4\text{DSCD}}}{[O_4]_{\text{surface}}} \cdot f + c} \quad (1)$$

Where X_{DSCD} and $O_{4\text{DSCD}}$ are the slant measured columns of the species X and O_4 , respectively. $[O_4]_{\text{surface}}$ is the O_4 at the level of the station, f is the correction factor due to differences in wavelength ranges of the specie under study with respect to O_4 that can be computed from a radiative transfer model (RTM) and c is the error of the approach. The later is a factor accounting for the dependence with the different vertical distributions of both species and AMFs.

$$c = h(Rg - R'g') \quad (2)$$

h is the effective scattering height of the vertical ray. R and R' are the ratio of the mean concentration of the layer divided by the concentration at the level of the station of tracer X and O_4 , respectively, and g and g' accounts for the AMF ($g = \text{AMF}(\text{SZA}) - 1$), where SZA stands for Solar Zenith Angle.

The effective scattering height is defined as

$$h(z) = \sum_{\text{surface}}^{\text{top}} \left(\frac{I(z)}{\int_{\text{surface}}^{\text{top}} I(z) dz} z \right) \quad (3)$$

where
$$\frac{I(z)}{\int_{\text{surface}}^{\text{top}} I(z) dz}$$

represents the normalized contribution of the ray scattered at each atmospheric layer to the total flux at surface. From radiative transfer calculations it can be shown that the effective scattering height ranges between 6.5 and 7.5 km above the station for solar zenith angle (SZA) below 70° , which we estimate as the validity limit of the method.

NO₂ seasonal evolution in the North Subtropical free troposphere

M. Gil-Ojeda et al.

Title Page

Abstract

Introduction

Conclusions

References

Tables

Figures

◀

▶

◀

▶

Back

Close

Full Screen / Esc

Printer-friendly Version

Interactive Discussion



NO₂ seasonal evolution in the North Subtropical free troposphere

M. Gil-Ojeda et al.

Title Page

Abstract

Introduction

Conclusions

References

Tables

Figures

◀

▶

◀

▶

Back

Close

Full Screen / Esc

Printer-friendly Version

Interactive Discussion



Since both NO₂ and O₄ are analyzed in the same spectral range, the difference between the weighted center of the range for NO₂, i.e. the effective wavelength, and that of O₄ is small. The value of f is of 0.9 for a near-Rayleigh atmosphere.

By using Eq. (2), the error introduced in NO₂ vmr due to the geometrical approximation, if assuming a constant mixing ratio of both O₄ and NO₂ with height, is of 9% at 70° SZA and of 2.3% at 50° SZA. Since the scattering heights and the air mass factors are well known, the data can be corrected. The only uncertainty is due to the R value related to the vertical distribution of NO₂ within the FT. However, aircraft measurements over the ocean far from large industrial areas show that the tropospheric vertical distribution is nearly constant above the MBL (Bucsela et al., 2008).

In the presence of moderate or high aerosols loading at the level of the observational point, multiple scattering takes place and the method is no longer valid. Assuming that the aerosol layer is a well mixed layer, we estimate the AOD = 0.1 at 500 nm as a safe limit (Gomez et al., 2014).

Since the path length is obtained from O₄ measurements, uncertainty in the magnitude of its absolute cross section is an additional source of error. It has been reported that paths obtained from O₄ are even larger than that RT computed for a Rayleigh atmosphere (Wagner et al., 2002) when using the generally accepted cross-sections reported in literature (Greenblatt, 1990; Hermans et al., 1999), suggesting that cross-section are underestimated. There is, however, no agreement in the magnitude of the correct values. We performed direct Sun measurements on a very clear morning (Aerosol Optical Density at 500 nm over the observatory = 0.007 ± 0.00077) at an O₄ effective temperature of 250 K, and compared the retrieved slants columns with the ones calculated from the local radiosounding of the day (7 October 2014) up to 30 km and the tropical standard atmosphere from 30 km upwards. Results show an excellent agreement with no difference at the error level when the retrieval includes O₄ cross-sections at two temperatures (Fig. 1). In this exercise, the Thalman and Volkamer (2013) cross-sections at 203 and 293 K were used. When including only the room temperature cross-section in the retrieval, the obtained O₄ is 3–5% too large.

NO₂ seasonal evolution in the North Subtropical free troposphere

M. Gil-Ojeda et al.

[Title Page](#)[Abstract](#)[Introduction](#)[Conclusions](#)[References](#)[Tables](#)[Figures](#)[Back](#)[Close](#)[Full Screen / Esc](#)[Printer-friendly Version](#)[Interactive Discussion](#)

Our results agree with the very recent report by Spinei et al. (2014) who found a temperature dependence of 9 % for a variation of 44 K and no pressure dependence based on direct sun and aircraft MAXDOAS measurements. The conclusion of their work is that no corrections need to be made for effective temperatures near 275 K. Since the present method uses only the horizontal path, the temperature along the path is nearly constant and the seasonal variability in the subtropical FT is small. Air temperature at the level of Izaña ranges from 277 K in January–February to 287 K in July–August. Consequently, no more than 2 % of error is expected due to this effect.

Typical NO₂ SCD root mean square error of the fit for horizontal geometry is of 3×10^{14} molec cm⁻². These errors represent 15–20 % of the typical differential SCD. A summary of the analysis errors is shown in Table 1.

3 The Izaña observatory and dataset

Izaña (28.3° N, 16.5° W) is a well known GAW-NDACC station located at the top of the Izaña mountain, one of the peaks of the great crater of the Teide volcano, at 2370 m a.s.l., in Tenerife Island. The observatory and related meteorology has been extensively described in previous publications (i.e. Rodriguez et al., 2009; Cuevas et al., 2013). It is representative of the FT at night. During daytime it is frequently affected by anabatic winds resulting from heating of the ground. This upslope breeze carries boundary layer air masses to the FT. The intensity of the wind peaks near the local noon and can extend well into the afternoon. It can be indirectly quantified using the measurements of water vapour on the station since air masses from below carry high humidity to the height of the observatory. The measurements of in-situ NO₂ are also useful for this purpose, since the BL NO₂ concentrations in populated areas near the coast are typically more than one order of magnitude larger than the background FT.

For the present work only the horizontal spectra are analyzed. If the SZA was lower than 10°, then the 70° elevation spectrum was used as reference to avoid spectral

distortions due to too short integration times. In all other cases the reference was the zenith spectrum of the same cycle.

Data from three complete years (2011–2013) have been used after screening for (a) NO₂ RMSE: fit error is limited to 2×10^{15} molec_{cc}cm⁻² and a signal to noise ratio of 0.5, which is approximately the detection limit of the instrument. (b) High SZA: only data corresponding to data below SZA 70° are used in the present analysis to limit the error in the path calculations. (c) Aerosol loading: measurements on days with Aerosol Optical Depth (AOD) at 500 nm over 0.1, were rejected. (d) Length of the path: individual measurements with paths shorter than 30 km were also rejected (broken clouds or narrow dust layers might cause this effect). (e) Unrealistic negative values appearing occasionally: over 15.000 of data passed all filters for the 3 years period (40 % of all possible data).

4 The Optimal Estimation Method

The Optical Estimation Method (OEM) has been extensively used on last years to obtain NO₂ vertical profiles on moderate to high polluted environments. However, on free troposphere background conditions, the concentrations are near the instrumental detection limit (10–100 pptv) and in these conditions the method provide unrealistic profiles. In this work we have used it only to characterize the vertical distribution of the plume in a particular case study in which a high NO₂ airmass arrived to the station.

In the OEM formalism (Rodgers, 2000) the most probable vertical distribution $\hat{\mathbf{x}}$ is given by

$$\hat{\mathbf{x}} = \mathbf{x}_a + \mathbf{S}_a \mathbf{K}^T (\mathbf{K} \mathbf{S}_a \mathbf{K}^T + \mathbf{S}_\varepsilon)^{-1} (\mathbf{y} - \mathbf{K} \mathbf{x}_a)$$

Where \mathbf{y} is a set of measurements with the errors covariance \mathbf{S}_ε . The weighting functions matrix \mathbf{K} express the sensitivity of the measurements to variations in the trace gas profile and is obtained with the SPSPDISORT pseudo-spherical radiative transfer solver

NO₂ seasonal evolution in the North Subtropical free troposphere

M. Gil-Ojeda et al.

Title Page

Abstract

Introduction

Conclusions

References

Tables

Figures



Back

Close

Full Screen / Esc

Printer-friendly Version

Interactive Discussion



NO₂ seasonal evolution in the North Subtropical free troposphere

M. Gil-Ojeda et al.

Title Page

Abstract

Introduction

Conclusions

References

Tables

Figures

◀

▶

◀

▶

Back

Close

Full Screen / Esc

Printer-friendly Version

Interactive Discussion



128/2013, obtained by using the OEM technique (Rodgers, 2000), indicating that the enhancement takes place near the level of the station, with an upper limit around 4 km. This confirms that once the air mass passes over the mountain obstacle it either moves horizontally or descends again but remaining in the FT. Note that the instrument scanning lowest angle is below the horizon ($IEA = -1^\circ$), thus containing information about the trace gas concentration below the station.

It is worth to mention that Southern winds are generally related to African air masses containing Saharan dust and, as previously mentioned, those dusty days were filtered out from the analysis. The only non-dusty south wind cases observed are from Atlantic airmasses which suffered an abrupt change in direction when approaching to Africa. Consequently the impact of this effect on the overall dataset is small. Only five clear cases have been identified within the 3 year record. Those cases have been removed for seasonal evolution studies.

Figure 4 (top panel) shows the NO₂ vmr seasonal evolution separated by year. The seasonal behavior is similar in all three years, with the maximum in the summer months and the minimum in winter time. Summer gaps result from the large number of Saharan dust intrusions during these months. To explore a possible dependence of the retrieved concentrations with the SZA, the data have been plotted in colors according the SZA (Fig. 4, mid panel). The maxima in summer months are observed regardless the SZA excluding the possibility of stratospheric contamination or any other SZA dependent artifact. The magnitudes of the retrieved concentration are also independent of the RMSE (Fig. 4, lower panel). Sporadic peaks over 100 pptv are observed with no increase in typical retrieval errors. The scattering along the day is also large with SDs of 10–15 pptv.

Monthly means clearly show the rapid spring build-up and the autumn decay (Fig. 5). Mean values range from 20 to 44 pptv throughout the year. A summer maximum has previously been found in unpolluted continental China in the boundary layer as result of soil biogenic NO emissions (Van der A et al., 2006; Qi et al., 2014). However, NO₂ in long paths over the Atlantic FT cannot be explained in this way. The output of the

twofold increase in the background NO₂ vmr. For instance, for a layer of 200 m with a NO₂ load of as high as 600 ppt would represent an increase in the column of some 5–10 % of the background concentration for a clean day.

We have recalculated NO₂ monthly means only from the first morning data, namely data between SZA 70° a.m. and 65° a.m. These SZA correspond to fractional days ranging from 0.42 in mid winter to 0.32 in summer. At this early time of day the anabatic wind is still under the first stage of development and the intensity of the upwelling is of only a few percent of the maximum value after noon. Results show that the seasonality in the SZA 65° to 70° data is almost identical than that when considering data at all SZA (ratio > 0.98). We therefore conclude that the summer increase is not a result of the contamination by high NO₂ upwelled MBL air masses.

6.1.2 Changes in horizontal transport patterns along season

Val Martin et al. (2008) analysed NO₂ mountain data from Azores and reported larger summer concentrations attributed to North American biomass burning. However, circulation at the lower latitudes than the Canary Island is quite different. Attempts to determine the global FT distribution of NO₂, based on the cloud slicing technique, have recently been made with OMI data (Choi et al., 2014), however the method does not provide results in summer over the Sahara region due to lack of cloudiness.

HYSPLIT 7 days backtrajectory cluster analysis shows that airmasses arriving to Izaña during the reporting period are fundamentally of Atlantic origin, with a small portion arriving from Africa during the summer period (Fig. 6), in agreement with the 22 year (1988–2009) backward trajectory climatology reported by Cuevas et al. (2013). As previously mentioned, only NO₂ observations under no-dust conditions are considered, therefore days with African trajectories are not included in the analysis. Winter trajectories are longer than the summer ones and 30 % of them cross the United States. All trajectory clusters show a steady descendent transport in the last 96 h prior to the arrival to Izaña and are originated at an altitude of 4000–5500 m.a.s.l.

**NO₂ seasonal
evolution in the North
Subtropical free
troposphere**

M. Gil-Ojeda et al.

Title Page

Abstract

Introduction

Conclusions

References

Tables

Figures



Back

Close

Full Screen / Esc

Printer-friendly Version

Interactive Discussion



Gomez, L., Navarro-Comas, M., Puentedura, O., Gonzalez, Y., Cuevas, E., and Gil-Ojeda, M.: Long-path averaged mixing ratios of O₃ and NO₂ in the free troposphere from mountain MAX-DOAS, *Atmos. Meas. Tech.*, 7, 3373–3386, doi:10.5194/amt-7-3373-2014, 2014.

Granier, C., Guenther, A., Lamarque, J. F., Mieville, A., Muller, J., Olivier, J., Orlando, J., Peters, J., Petron, G., Tyndall, G., and Wallens, S.: POET, a database of surface emissions of ozone precursors, available at at: <http://www.aero.jussieu.fr/projet/ACCENT/POET.php> (last access: 19 May 2015) 2005.

Heland, J., Schlanger, H., Richter, A., and Burrows, J. P.: First comparison of tropospheric NO₂ column densities retrieved from GOME measurements and in situ aircraft profile measurements, *Geophys. Res. Lett.*, 29, 1983, doi:10.1029/2002GL015528, 2002.

Hermans, C.: O₄ absorption cross-sections at 298 K (335.59–666.63 nm), available at: <http://spectrolab.aeronomie.be/index.htm> (last access: 19 May 2015), 2011.

Hilboll, A., Richter, A., and Burrows, J. P.: Long-term changes of tropospheric NO₂ over megacities derived from multiple satellite instruments, *Atmos. Chem. Phys.*, 13, 4145–4169, doi:10.5194/acp-13-4145-2013, 2013.

Hudman, R. C., Jacob, D. J., Turquety, S., Leibensperger, E. M., Murray, L. T., Wu, S., Gilliland, A. B., Avery, M., Bertram, T. H., Brune, W., Cohen, R. C., Dibb, J. E., Flocke, F. M., Fried, A., Holloway, J., Neuman, J. A., Orville, R., Perring, A., Ren, X., Sachse, G. W., Singh, H. B., Swanson, A., and Wooldridge, P. J.: Surface and lightning sources of nitrogen oxides over the United States: magnitudes, chemical evolution, and outflow, *J. Geophys. Res.*, 112, D12S05, doi:10.1029/2006JD007912, 2007.

Irie, H., Sudo, K., Akimoto, H., Richter, A., Burrows, J. P., Wagner, T., Wenig, M., Beirle, S., Kondo, Y., Sinyakov, V. P., and Goutail, F.: Evaluation of long-term tropospheric NO₂ data obtained by GOME over East Asia in 1996–2002, *Geophys. Res. Lett.*, 32, L11810, doi:10.1029/2005GL022770, 2005.

Jacob, D. J., Crawford, J. H., Kleb, M. M., Connors, V. S., Bendura, R. J., Raper, J. L., Sachse, G. W., Gille, J. C., Emmons, L., and Heald, C. L.: Transport and Chemical Evolution over the Pacific (TRACE-P) aircraft mission: design, execution, and first results, *J. Geophys. Res.*, 108, 9000, doi:10.1029/2002JD003276, 2003.

Lamarque, J.-F., Emmons, L. K., Hess, P. G., Kinnison, D. E., Tilmes, S., Vitt, F., Heald, C. L., Holland, E. A., Lauritzen, P. H., Neu, J., Orlando, J. J., Rasch, P. J., and Tyndall, G. K.: CAM-chem: description and evaluation of interactive atmospheric chemistry in the Community Earth System Model, *Geosci. Model Dev.*, 5, 369–411, doi:10.5194/gmd-5-369-2012, 2012.

NO₂ seasonal evolution in the North Subtropical free troposphere

M. Gil-Ojeda et al.

Title Page

Abstract

Introduction

Conclusions

References

Tables

Figures



Back

Close

Full Screen / Esc

Printer-friendly Version

Interactive Discussion

Lamsal, L. N., Martin, R. V., van Donkelaar, A., Celarier, E. A., Bucsela, E. J., Boersma, K. F., Dirksen, R., Luo, C., and Wang, Y.: Indirect validation of tropospheric nitrogen dioxide retrieved from the OMI satellite instrument: insight into the seasonal variation of nitrogen oxides at northern midlatitudes, *J. Geophys. Res.*, 115, D05302, doi:10.1029/2009JD013351, 2010.

Mayer, B. and Kylling, A.: Technical note: The libRadtran software package for radiative transfer calculations – description and examples of use, *Atmos. Chem. Phys.*, 5, 1855–1877, doi:10.5194/acp-5-1855-2005, 2005.

Ordóñez, C., Lamarque, J.-F., Tilmes, S., Kinnison, D. E., Atlas, E. L., Blake, D. R., Sousa Santos, G., Brasseur, G., and Saiz-Lopez, A.: Bromine and iodine chemistry in a global chemistry-climate model: description and evaluation of very short-lived oceanic sources, *Atmos. Chem. Phys.*, 12, 1423–1447, doi:10.5194/acp-12-1423-2012, 2012.

Parrish, D. D., Ryerson, T. B., Holloway, J. S., Neuman, J. A., Roberts, J. M., Williams, J., Stroud, C. A., Frost, G. J., Trainer, M., Hübler, G., Fehsenfeld, F. C., Flocke, F., and Weinheimer, A. J.: Fraction and composition of NO_y transported in air masses lofted from the North American continental boundary layer, *J. Geophys. Res.*, 109, D09302, doi:10.1029/2003JD004226, 2004.

Persson, A. and Grazzini, F.: User Guide to ECMWF forecast products, Meteorological Bulletin M3.2, edited by: ECMWF, available at: http://www.uio.no/studier/emner/matnat/geofag/GEF4220/v09/undervisningsmateriale/Persson_user_guide.pdf (last access: 19 May 2015), updated 2007.

Puentedura, O., Gil, M., Saiz-Lopez, A., Hay, T., Navarro-Comas, M., Gómez-Pelaez, A., Cuevas, E., Iglesias, J., and Gomez, L.: Iodine monoxide in the north subtropical free troposphere, *Atmos. Chem. Phys.*, 12, 4909–4921, doi:10.5194/acp-12-4909-2012, 2012.

Qi, Y.: Spatio-temporal distributions of tropospheric NO₂ over oases in Taklimakan Desert, China, *Chinese Geogr. Sci.*, 1–8, doi:10.1007/s11769-014-0696-z, 2014.

Reidmiller, D. R., Jaffe, D. A., Fischer, E. V., and Finley, B.: Nitrogen oxides in the boundary layer and free troposphere at the Mt. Bachelor Observatory, *Atmos. Chem. Phys.*, 10, 6043–6062, doi:10.5194/acp-10-6043-2010, 2010.

Richter, A., Burrows, J. P., Nüs, H., Granier, C., and Niemeier, U.: Increase in tropospheric nitrogen dioxide over China observed from space, *Nature*, 437, 129–132, doi:10.1038/nature04092, 2005.

NO₂ seasonal evolution in the North Subtropical free troposphere

M. Gil-Ojeda et al.

Title Page

Abstract

Introduction

Conclusions

References

Tables

Figures



Back

Close

Full Screen / Esc

Printer-friendly Version

Interactive Discussion

Ridley, B. A., Carroll, M. A., Gregory, G. L., and Sachse, G. W.: NO and NO₂ in the troposphere: technique and measurements in regions of a folded tropopause, *J. Geophys. Res.*, 93, 15813–15830, 1988.

Rodgers, C. D.: *Inverse Methods for Atmospheric Sounding: Theory and Practice*, vol. 2, Atmospheric, Oceanic and Planetary Physics, World Scientific, Hackensack, NJ, doi:10.1142/9789812813718_fmatter, 2000.

Rodríguez, S., González, Y., Cuevas, E., Ramos, R., Romero, P. M., Abreu-Afonso, J., and Redondas, A.: Atmospheric nanoparticle observations in the low free troposphere during upward orographic flows at Izaña Mountain Observatory, *Atmos. Chem. Phys.*, 9, 6319–6335, doi:10.5194/acp-9-6319-2009, 2009.

Saiz-Lopez, A., Lamarque, J.-F., Kinnison, D. E., Tilmes, S., Ordóñez, C., Orlando, J. J., Conley, A. J., Plane, J. M. C., Mahajan, A. S., Sousa Santos, G., Atlas, E. L., Blake, D. R., Sander, S. P., Schauffler, S., Thompson, A. M., and Brasseur, G.: Estimating the climate significance of halogen-driven ozone loss in the tropical marine troposphere, *Atmos. Chem. Phys.*, 12, 3939–3949, doi:10.5194/acp-12-3939-2012, 2012.

Schultz, M., Schmitt, R., Thomas, K., and Volz-Thomas, A.: Photochemical box modeling of long-range transport from North America to Tenerife during the North Atlantic Regional Experiment (NARE) 1993, *J. Geophys. Res.*, 103, 13477–13488, doi:10.1029/97JD01481, 1998.

Spinei, E., Cede, A., Herman, J., Mount, G. H., Eloranta, E., Morley, B., Baidar, S., Dix, B., Ortega, I., Koenig, T., and Volkamer, R.: Ground-based direct-sun DOAS and airborne MAX-DOAS measurements of the collision-induced oxygen complex, O₂O₂, absorption with significant pressure and temperature differences, *Atmos. Meas. Tech.*, 8, 793–809, doi:10.5194/amt-8-793-2015, 2015.

Stunder, B.: An assessment of the quality of forecast trajectories, *J. Appl. Meteorol.*, 35, 1319–1331, 1996.

Thalman, R. and Volkamer, R. Temperature dependent absorption cross-sections of O₂–O₂ collision pairs between 340 and 630 nm and at atmospherically relevant pressure, *Phys. Chem. Chem. Phys.*, 15, 15371–15381, doi:10.1039/c3cp50968k, 2013.

Val Martin, M., Honrath, R. E., Owen, R. C., and Li, Q. B.: Seasonal variation of nitrogen oxides in the central North Atlantic lower free troposphere, *J. Geophys. Res.*, 113, D17307, doi:10.1029/2007JD009688, 2008.

NO₂ seasonal evolution in the North Subtropical free troposphere

M. Gil-Ojeda et al.

Title Page

Abstract

Introduction

Conclusions

References

Tables

Figures



Back

Close

Full Screen / Esc

Printer-friendly Version

Interactive Discussion



- Vandaele, A. C., Hermans, C., Simon, P. C., Carleer, M., Colins, R., Fally, S., Mérienne, M. F., Jenouvrier, A., and Coquart, B.: Measurements of the NO₂ absorption cross-sections from 42 000 cm⁻¹ to 10 000 cm⁻¹ (238–1000 nm) at 220 and 294 K, *J. Quant. Spectrosc. Ra.*, 59, 171–184, doi:10.1016/S0022-4073(97)00168-4, 1998.
- 5 Van der A, R. J., Peters, D. H. M. U., Eskes, H., Boersma, K. F., Van Roozendael, M., De Smedt, I., and Kelder, H. M.: Detection of the trend and seasonal variation in tropospheric NO₂ over China, *J. Geophys. Res.*, 111, D12317, doi:10.1029/2005JD006594, 2006.
- Wagner, T., von Friedeburg, C., Wening, M., Otten, C., and Platt, U.: UV-Visible observations of atmospheric O₄ absorptions using direct moonlight and zenith-scattered sunlight for clear sky and cloudy sky conditions, *J. Geophys. Res.*, 107, 4424, doi:10.1029/2001JD001026, 2002.
- Wagner, T., Dix, B., Friedeburg, C. V., Friess, U., Sinreich, R., and Platt, U.: MAX-DOAS O₄ measurements: a new technique to derive information on atmospheric aerosols – principles and information content, *J. Geophys. Res.*, 109, D22205, doi:10.1029/2004JD004904, 2004.
- 15 Wenger, R.: Zur Theorie der Berg- und Talwinde, *Meteorol. Z.*, 7, 193–204, 1923.
- Wittrock, F., Oetjen, H., Richter, A., Fietkau, S., Medeke, T., Rozanov, A., and Burrows, J. P.: MAX-DOAS measurements of atmospheric trace gases in Ny-Ålesund – Radiative transfer studies and their application, *Atmos. Chem. Phys.*, 4, 955–966, doi:10.5194/acp-4-955-2004, 2004.
- 20 Ziemke, J. R., Chandra, S., and Bhartia, P. K.: “Cloud slicing”: a new technique to derive upper tropospheric ozone from satellite measurements, *J. Geophys. Res.*, 106, 9853–9867, 2001.
- Zien, A. W., Richter, A., Hilboll, A., Blechschmidt, A.-M., and Burrows, J. P.: Systematic analysis of tropospheric NO₂ long-range transport events detected in GOME-2 satellite data, *Atmos. Chem. Phys.*, 14, 7367–7396, doi:10.5194/acp-14-7367-2014, 2014.

NO₂ seasonal evolution in the North Subtropical free troposphere

M. Gil-Ojeda et al.

Table 1. Method uncertainty.

Uncertainty in NO ₂ due to fit	15–20 %
Uncertainty in path due to the O ₄ fit	< 1 %
Uncertainty of the method (related to unknown vertical distribution of NO ₂ and actual effective path)	2.5–9 % (for sza: 50 to 70°)
Error in horizontal path due to O ₄ cross-sections temperature dependence	2 %
Overall uncertainty	20–32 %

Title Page

Abstract

Introduction

Conclusions

References

Tables

Figures



Back

Close

Full Screen / Esc

Printer-friendly Version

Interactive Discussion



NO₂ seasonal evolution in the North Subtropical free troposphere

M. Gil-Ojeda et al.

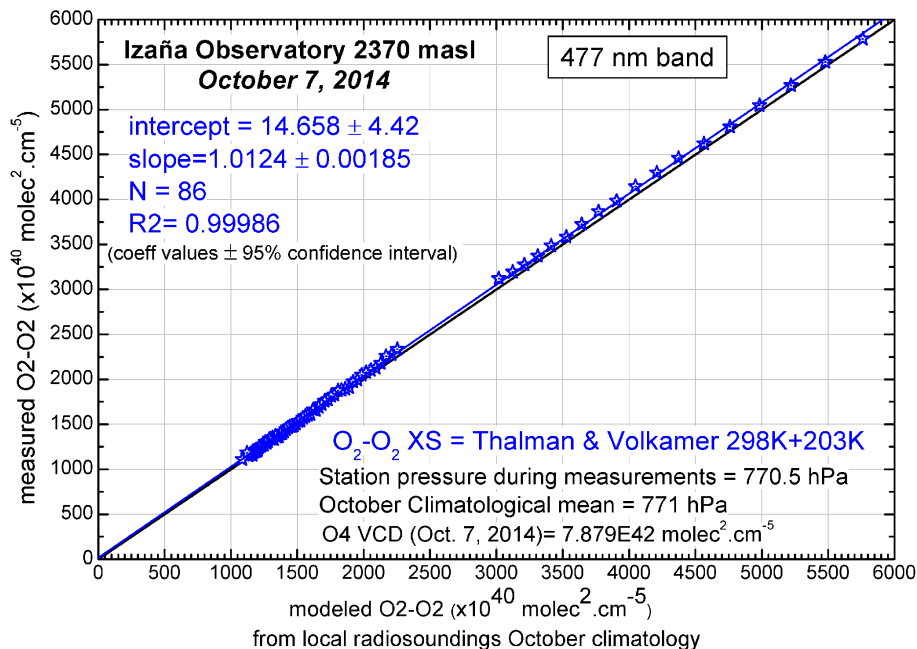


Figure 1. Measured O₄ SCD vs. modeled O₄ for a pure Rayleigh atmosphere at the 477 nm band by using cross-sections at 203 and 293 K temperatures (see text for details).

Title Page

Abstract

Introduction

Conclusions

References

Tables

Figures

◀

▶

◀

▶

Back

Close

Full Screen / Esc

Printer-friendly Version

Interactive Discussion



NO₂ seasonal evolution in the North Subtropical free troposphere

M. Gil-Ojeda et al.

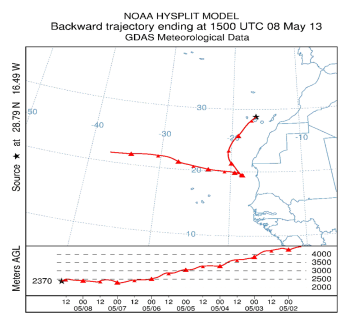
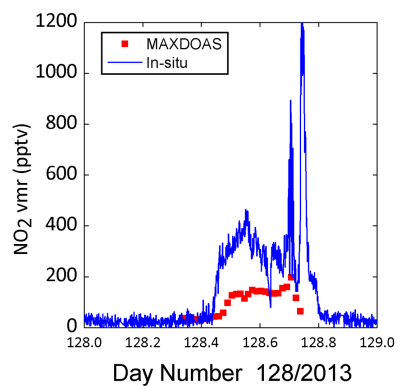
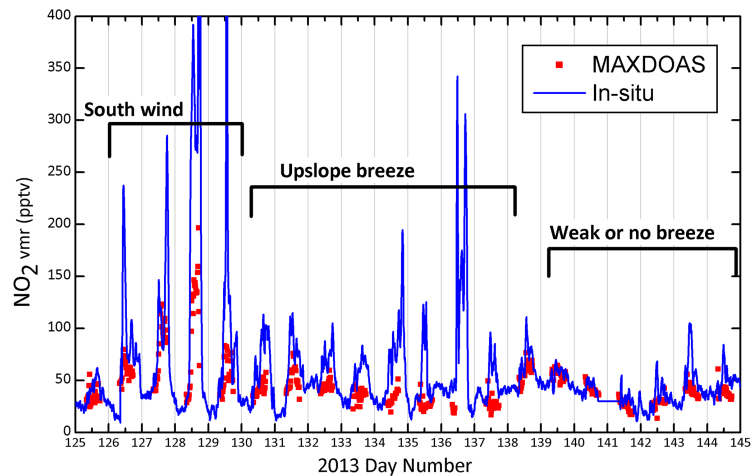


Figure 2. Izaña MAXDOAS vs. minutal in-situ NO₂ volume mixing ratio for a period of time representative of 3 different wind situation. In-situ data are smoothed by 50 min running mean (top panel). Expanded plot for day 8 May 2013 (day number 128). Backtrajectory ending at Izaña at 15 h of the same day.

Title Page

Abstract Introduction

Conclusions References

Tables Figures

◀ ▶

◀ ▶

Back Close

Full Screen / Esc

Printer-friendly Version

Interactive Discussion



NO₂ seasonal evolution in the North Subtropical free troposphere

M. Gil-Ojeda et al.

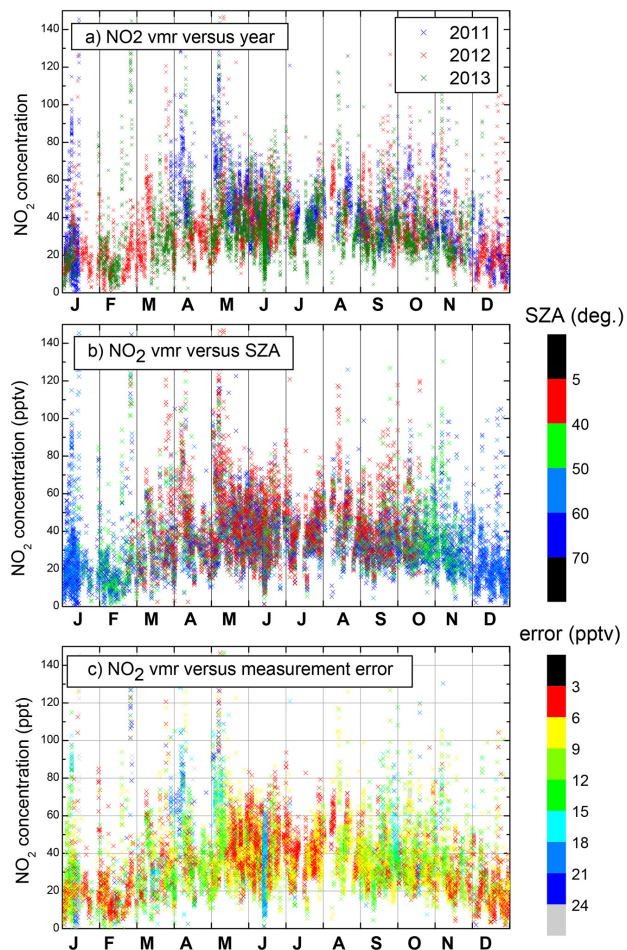


Figure 4. Seasonal evolution of the individual data NO₂ vmr separated by years (upper panel). Separated by Solar Zenith Angles (mid panel) and separated by RMSE (lower panel).

Title Page

Abstract Introduction

Conclusions References

Tables Figures

◀ ▶

◀ ▶

Back Close

Full Screen / Esc

Printer-friendly Version

Interactive Discussion



NO₂ seasonal evolution in the North Subtropical free troposphere

M. Gil-Ojeda et al.

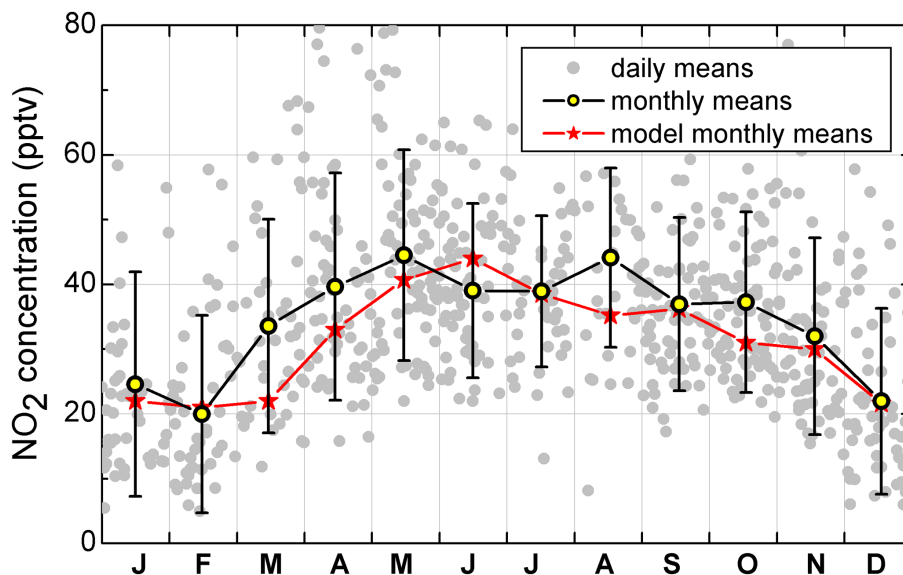


Figure 5. NO₂ concentration monthly means at the level of Izaña Observatory with their respective SDs (open circles and black lines). CAM-Chem model results for the same level are shown for comparison (Red stars and lines). Individual solid grey circles are the 3 years diurnal mean.

[Title Page](#)[Abstract](#)[Introduction](#)[Conclusions](#)[References](#)[Tables](#)[Figures](#)[◀](#)[▶](#)[◀](#)[▶](#)[Back](#)[Close](#)[Full Screen / Esc](#)[Printer-friendly Version](#)[Interactive Discussion](#)

NO₂ seasonal evolution in the North Subtropical free troposphere

M. Gil-Ojeda et al.

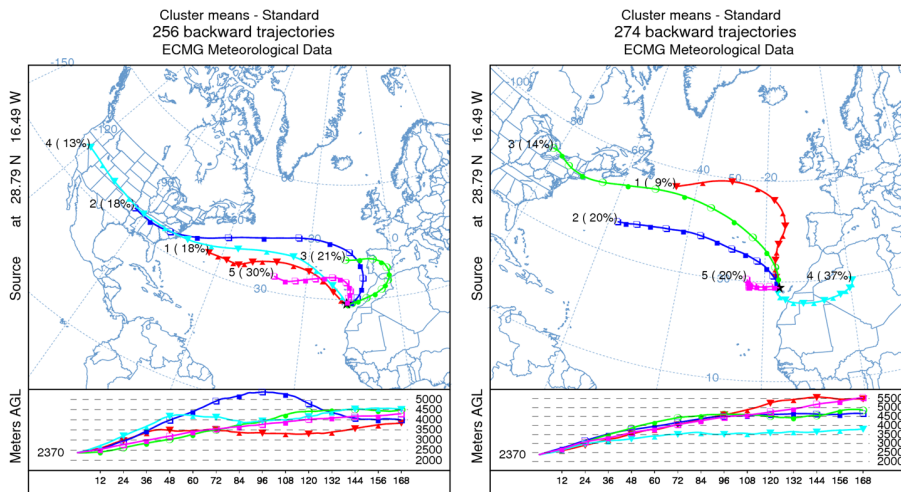


Figure 6. 1 week HYSPLIT backtrajectories clusters arriving to Izaña Observatory for the summer months (JJA) and years 2011–2013.

Title Page

Abstract

Introduction

Conclusions

References

Tables

Figures

◀

▶

◀

▶

Back

Close

Full Screen / Esc

Printer-friendly Version

Interactive Discussion



NO₂ seasonal evolution in the North Subtropical free troposphere

M. Gil-Ojeda et al.

Title Page

Abstract

Introduction

Conclusions

References

Tables

Figures



Back

Close

Full Screen / Esc

Printer-friendly Version

Interactive Discussion

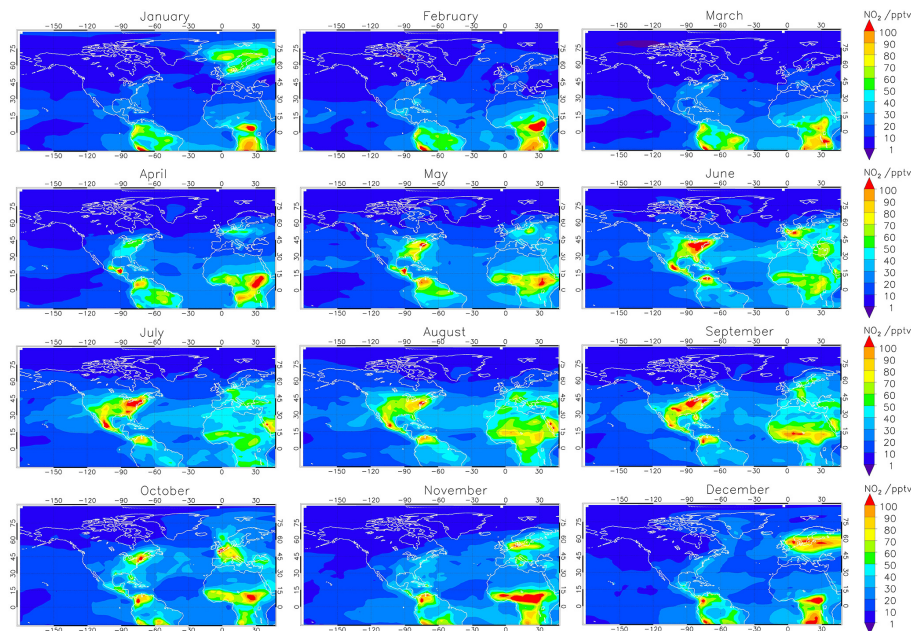


Figure 7. Global distributions of monthly mean NO₂ vmr for the level 5.9 km obtained from the Cam-CHEM chemistry climate model-model.

NO₂ seasonal evolution in the North Subtropical free troposphere

M. Gil-Ojeda et al.

Title Page

Abstract

Introduction

Conclusions

References

Tables

Figures

◀

▶

◀

▶

Back

Close

Full Screen / Esc

Printer-friendly Version

Interactive Discussion

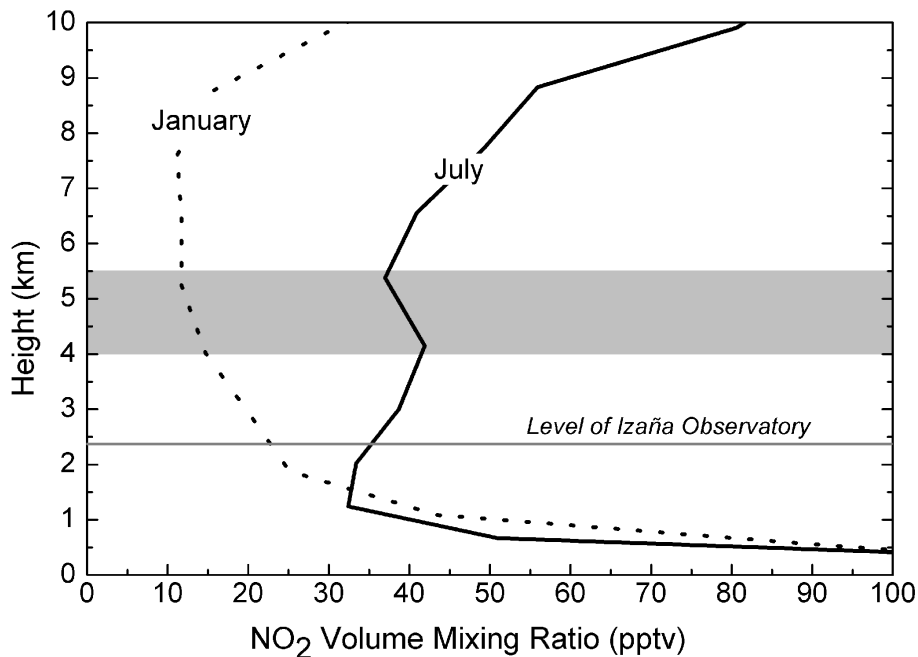


Figure 8. NO₂ vmr monthly means vertical profiles from Cam-CHEM model. Gray band represents the height range where airmasses are originated (see text).